High Helicities of Lys-Containing, Ala-Rich Peptides Are Primarily Attributable to a Large, Context-Dependent Lys Stabilization

Lawrence Williams, Kristian Kather, and D. S. Kemp*

Contribution from the Department of Chemistry, Room 18−582, Massachusetts Institute of Technology, Cambridge, Massachusetts 02139

Received January 20, 1998

Abstract: Peptides 1K, YKGGGAAAAAAAAKAAAAAAAAAAGGGK-NH_2; 2K, YKGGGAAAAAKAAAAA-KAAAAAAGGGK-NH_2; and 3K, YKGGGAAAAKAAAAKAAAAKAAAGGGK-NH_2 have been prepared by solid-phase synthesis, purified, and characterized by amino acid analysis, MALDI mass spectrometry, and ultracentrifugation. Their circular dichroism (CD) spectra of unaggregated solutions are reported for measurements in 0.01 M NaCl at 2, 25, and 60 °C and at 2 °C in aqueous guanidinium hydrochloride (0−3 M) and aqueous trifluoroethanol (TFE, 0−15 mol %). The CD spectra exhibit a helical signature in 0.01 M NaCl or in water−TFE at 2 °C, and the intensities of the mean residue ellipticities at the minimums of 222 nm in 0.01 M NaCl are (1K) −9100, (2K) −18 100, and (3K) −19 900 deg cm^{-1} $dmol^{-1}$. These ellipticities are accurately modeled using a Lifson−Roig algorithm by the helical propensities previously reported by Renold et al. (Renold, P.; Tsang, K.-Y.; Shimizu, L. S.; Kemp, D. S. *J. Am. Chem. Soc.* **1996**, *118*, 12234−12235.) but not by those of Doig and Baldwin (Doig, A. J.; Baldwin, R. L. *Protein Sci.* **1995**, *4*, 1325−1336.). The helicities of peptides such as 1K, 2K, and 3K are best attributed to a lysine stabilization and not to an intrinsic helix propensity of alanine.

Polypeptides vary dramatically in their tendency to assume α-helical conformations in water, and rigorous characterization of the dependence of helicity on amino acid composition and sequence poses a significant problem in chemical cryptography. The simplest of all helicity models postulates contributions from the intrinsic helical propensities (*s* or *w* values) of the component amino acids, each acting independently of its site on the peptide chain (site independence) and of its neighbors within the peptide sequence (context independence). Sets of *w* values assigned in different host peptides and proteins[1−7] exhibit significant correlations,[8−11] yet the agreement falls far short of the requirements for a quantitative helicity algorithm, and interpretations of these results remain controversial. Rigorous assignment of the helical propensity of alanine is pivotal. Although most recent studies rank alanine as the strongest helix former, we now show that lysine is primarily responsible for the high helix stabilization seen for the widely studied class of alanine-rich lysine-containing peptides.

Context independence has been criticized as a general model assumption.[12,13] For the particular case of amino acid residues bearing charged side chains, *w* values have been predicted[14] and shown[15−17] to be strongly site dependent (charge−helix dipole interaction). The relative importance of context- or site-dependent and context- and site-independent contributions to helicity is currently unknown, but an accurate helicity algorithm clearly must include mutually consistent coefficients that reflect all these contributions, which must be measured by site mutations in a host that is free of significant uncharacterized site or context effects. Context dependencies are particularly likely to arise through interactions between side chains of amino acids that appear within four contiguous residues of a peptide sequence, corresponding to a single loop of a peptide helix.

It is difficult to design a host that is free of context effects. As the helix-stabilizing amino acid with the least bulky nonpolar side chain, alanine might be presumed to minimize steric interactions with other residues within a helical loop, and polyalanine is a likely candidate for a minimally interactive host.

(1) O'Neil; K. T.; DeGrado, W. F. *Science* **1990**, *250*, 646−651.
(2) Lyu, P. C.; Liff, M. I.; Marky, L. A.; Kallenbach, N. R. *Science* **1990**, *250*, 669−673.
(3) Wojcik, J.; Altman, K. H.; Scheraga, H. A. *Biopolymers* **1990**, *30*, 121−134.
(4) Horwitz, A.; Matthews, J. M.; Fersht, A. R. *J. Mol. Biol.* **1992**, *227*, 560−568.
(5) Park, S.-H.; Shalongo, W.; Stellwagen, E. *Biochemistry* **1993**, *32*, 7048−7053.
(6) (a) Blaber, M.; Zhang, X.−j.; Matthews, B. W. *Science* **1993**, *260*, 1637−1640. (b) Blaber, M.; Zhang, X.−j.; Lindstrom, J. D.; Pepiot, S. D.; Baase, W. A.; Matthews, B. W. *J. Mol. Biol.* **1994**, *235*, 600−624.
(7) Chakrabartty, A.; Kortemme, T.; Baldwin, R. L. *Protein Sci.* **1994**, *3*, 843−852.
(8) Chakrabartty, A.; Baldwin R. L. *Adv. Protein Chem.* **1995**, *46*, 141−176.
(9) Creamer, T. P.; Rose, G. D. *Proteins: Struct. Funct. Genet.* **1994**, *19*, 85−97.
(10) Luque, I.; Mayorga, O. L.; Freire, E. *Biochemistry* **1996**, *35*, 13681−13688.
(11) Myers, J. K.; Pace, C. N.; Scholtz, J. M. *Proc. Natl. Acad. Sci. U.S.A.* **1997**, *94*, 2833−2837.
(12) Lesk, A. M. *Nature* **1991**, *352*, 379−380.
(13) Serrano, J.; Sancho, J.; Fersht, A. R. *Nature* **1992**, *356*, 453−455.
(14) (a) Vila, J.; Williams, R. L.; Grant, J. A.; Wojcik, J.; Scheraga, H. A. *Proc. Natl. Acad. Sci. U.S.A.* **1992**, *89*, 7821−7825. (b) Nemethy, G.; Scheraga, H. A. *J. Phys. Chem.* **1962**, *66*, 1773−1789. (c) Nemethy, G.; Steinberg, I. Z.; Scheraga, H. A. *Biopolymers* **1963**, *1*, 43−63. (d) Vásquez, M.; Pincus, M. R.; Scheraga, H. A. *Biopolymers* **1987**, *26*, 351−371. (e) Vásquez, M.; Scheraga, H. A. *Biopolymers* **1988**, *27*, 41−58.
(15) (a) Schoemaker, K. R.; Kim, P. S.; York, E. J.; Stewart, J. M.; Baldwin, R. L. *Nature* **1987**, *326*, 563−567. (b) Armstrong, K. M.; Baldwin, R. L. *Proc. Natl. Acad. Sci. U.S.A.* **1993**, *90*, 11337−11340. (c) Huyghues-Despointes, B. M. P.; Scholtz, J. M.; Baldwin, R. L. *Protein Sci.* **1993**, *3*, 1604−1611.
(16) Esposito, G.; Dhanapal, B.; Dumy, P.; Varma, V.; Mutter, M.; Bodenhausen, G. *Biopolymers* **1997**, *41*, 27−35.
(17) (a) Groebke, K.; Renold, P.; Tsang, K.-Y.; Allen. T. J.; McClure, K.; Kemp, D. S. *Proc. Natl. Acad. Sci. U.S.A.* **1996**, *93*, 2025−2029. (b) Renold, P.; Tsang, K.-Y.; Shimizu, L. S.; Kemp, D. S. *J. Am. Chem. Soc.* **1996**, *118*, 12234−12235. (c) Tsang, K.-Y.; Lee, J.; H.; Kemp, D. S. Unpublished results.

10.1021/ja9801947 CCC: $15.00
Published on Web 10/20/1998

Unfortunately, all but the shortest polyalanine sequences exhibit intractable aggregation, and for natural peptides, helicity can only be detected for sequences containing at least 15−20 amino acid residues. Aggregation in this size range can be minimized through introduction of solubilizing amino acid residues,[18] but these may create their own context dependencies. The solubilized alanine-rich hosts that are reported in the literature have not been subjected to rigorous tests to exclude or evaluate such dependencies.

We have recently developed a helical template Ac-Hel$_1$, a conformationally restricted derivative of Ac-L-Pro-L-Pro. When N-terminally linked to helically disposed polypeptides, Ac-Hel$_1$ initiates and strongly stabilizes α-helical conformations and allows NMR-based quantitation of their helicity.[19] By studying Ac-Hel$_1$ conjugates of short alanine-rich peptides (5−15 residues), we have characterized helices that are too unstable to be detected in the corresponding nontemplated peptides, and we have used them to characterize the stabilities of alanine-rich helices containing a single lysine residue.[17] The resulting helical propensities are inconsistent with others that have been recently reported. Explanations for this inconsistency include perturbations attributable to the template, as well as atypical features of short helical contexts, which necessarily contain a large fraction of amino acid residues in helical C- and N-terminal regions. Alternatively, context-dependent effects may have biased literature assignments of *w* values.

This controversy could be resolved through correlation of helicity for large nontemplated alanine-rich peptides that contain one or more lysines or other solubilizing residues, so spaced to minimize context effects. For three peptides that meet these conditions we now report helicities that validate our template-derived *w* values.

Host Contexts and Alanine-Rich Helical Peptides

Helical propensities have been recently assigned from studies of hosts that include oligopeptides,[3] small natural proteins,[4,6] helix bundles,[1] and unaggregated polypeptides.[2,5,7] With the exception of the thermal denaturation experiments carried out on functionalized polyglutamine oligopeptides by Scheraga and co-workers,[3] these studies rank alanine as the strongest helix former. The degree of dominance is strongly host-dependent. If for each host, the helical propensity of alanine is divided by the mean of the three highest propensities observed for other nonpolar amino acids, the ratios vary from 1.16 to 2.3,[5−7] suggesting the presence of large context sensitivities.

Two hosts were alanine-rich, lysine-containing peptides.[5,7] Among-medium sized polypeptides (15−25 residues) derived from the 20 natural amino acids, alanine-rich sequences that contain spaced Lys, Arg, Glu, or Gln residues form unusually stable helices near 0 °C in water,[20,21] and these are the simplest known peptides that exhibit both significant helicity and a minimum tendency toward aggregation. Since the report in 1989 by Marqusee, Robbins, and Baldwin,[20] the (Ala$_4$Lys)$_n$ peptides have been used for a variety of fundamental studies, including exploration of the length and sequence dependencies of the relative stabilities of α and 3_{10} helical conformations[22] and the intrahelical interactions of hydrophobic groups linked to Lys side chains.[23]

The cause of the high helicity of these Ala$_n$-Lys peptides remains unresolved. It has been modeled by two mutually exclusive w_{Ala} values, each paired with a corresponding value for w_{Lys}. For the first of these pairs, helicity is attributed to alanine;[7] for the second, echoing an earlier assignment by Scheraga,[3,14] helicity is attributed primarily to lysine in an alanine-rich context.[17] These assignments are not unique. When applied to a particular (Ala$_n$-Lys)$_m$ peptide, Lifson−Roig modeling[24] shows that any of a series of functionally dependent pairs of inversely correlated w_{Ala} and w_{Lys} values can be consistent with a particular fractional helicity.[25] Selecting one pair from this series requires further modeling of experimental helicities for a set of Ala-Lys peptides in which the Ala/Lys ratio varies significantly. The range of these ratios within the set defines the statistical precision with which the optimal w_{Ala}−w_{Lys} pair can be selected, but the selection is fundamentally invalid if significant context dependencies are present for some but not all set members. Proximate, charged lysine residues are particularly likely to generate such dependencies.

Baldwin and co-workers assigned a low w_{Lys} (0.82) and a high w_{Ala} (1.61) from studies of Ac-A$_4$KA$_4$KA$_4$KA-NH$_2$ and its analogues at 2 °C.[7] Their analysis relied on the observation that, for these peptides, replacement of Ala by Lys dramatically diminishes helicity,[20] and necessarily these replacements generated peptide sequences KA$_2$K and KAK, in which pairs of lysines appear at sites (i, i + 3) and (i, i + 2) within a helical loop.

We have shown by studies of short N-templated helical peptides that the stability of helices differs for otherwise similar peptides containing the KA$_2$K and KA$_4$K motifs.[17a,b] The latter exhibit much higher helicity and a larger temperature dependence of helicity. This observation has been extended to a larger data set,[17a,c] and we have attributed it to a context-dependent helix-destabilizing Lys−Lys interaction that is significant for KA$_2$K peptides but diminished or absent for KA$_4$K peptides, in which the pair of lysines lie outside of a helical loop.

From studies of N-templated alanine-rich peptides of varying length that contain a single lysine residue, we have assigned a low, nearly temperature independent w_{Ala} (1.07) and a high site-dependent w_{Lys} (1.25−5 at 25 °C) that is also diminished at high temperatures and by proximity to a second lysine residue.[17] The relevance of these assignments to larger, nontemplated peptides remains to be proven, and this issue can only be resolved through helicity comparisons between otherwise identical peptides that contain differing numbers of widely spaced Lys residues, for which context effects are expected to be minimal.

(18) Rothwart, D. M.; Davenport, V. G.; Shi, R. T.; Peng, J.-L.; Scheraga, H. A. *Biopolymers* **1996**, *39*, 531−536.

(19) (a) Kemp, D. S.; Allen, T. J.; Oslick, S. L. *J. Am. Chem. Soc.* **1995**, *117*, 6641−6657. (b) Kemp, D. S.; Allen, T. J.; Oslick, S. L.; Boyd, J. G. *J. Am. Chem. Soc.* **1996**, *118*, 4240−4248. (c) Kemp, D. S.; Oslick, S. L.; Allen, T. J. *J. Am. Chem. Soc.* **1996**, *118*, 4249−4255.

(20) Marqusee, S.; Robbins, V. H.; Baldwin, R. L. *Proc. Natl. Acad. Sci. U.S.A.* **1989**, *85*, 5286−5290.

(21) (a) Scholtz, J. M.; York, E. J.; Stewart, J. M.; Baldwin, R. L. *J. Am. Chem. Soc.* **1991**, *113*, 5102−5103. (b) Merutka, G.; Shalongo, W.; Stellwagen, E. *Biochemistry* **1991**, *30*, 4245−4248. (c) Shalongo, W.; Dugad, L.; Stellwagen, E. *J. Am. Chem. Soc.* **1994**, *116*, 8288−8293.

(22) (a) Fiori, W. R.; Miick, S. M.; Millhauser, G. L. *Biochemistry* **1993**, *32*, 11957−11962. (b) Fiori, W. R.; Lundberg, K. M.; Millhauser, G. L. *Nature Struct. Biol.* **1994**, *6*, 374−377.

(23) Albert, J. S.; Hamilton, A. D. *Biochemistry* **1995**, *34*, 984−990.

(24) (a) Qian, H.; Schellman, J. A. *J. Phys. Chem.* **1992**, *96*, 3987−3994. (b) Doig, A. J.; Chakrabartty, A.; Klingler, T. M.; Baldwin, R. L. *Biochemistry* **1994**, *33*, 3396−3403. (c) Doig, A. J.; Baldwin, R. L. *Protein Sci.* **1995**, *4*, 1325−1336.

(25) Using the standard Doig parameters (see Experimental Section) the Lifson−Roig fractional helicity for H−YKG$_3$A$_4$KA$_4$KA$_4$KA$_3$-G$_3$K-NH$_2$ can be shown to be consistent with w values of Chakrabartty et al.[7] (w_{Lys} = 0.82; w_{Ala} = 1.61) and of Renolds et al.[17b] (w_{Lys} = 5.3; w_{Ala} = 1.07) if $w_{Lys}(w_{Ala})^{4.584}$ = 7.196. A third consistent solution is w_{Lys} = w_{Ala} = 1.42. The two helicity propensities s and w are related by, $w = s(1 + v)$, where v = 0.048.

Design of Test Peptides

To test the validity of literature *w* values, five conditions must be met by a set of peptides containing an alanine-rich, lysine-containing core: (1) The alanine/lysine ratio within the set must vary significantly, but the core length must be constant, since helical stability depends strongly on peptide length, and the relationship between fractional helicity and CD ellipticity also shows significant length dependence. Most peptide set members thus must contain multiple lysine residues. (2) Lysine pairs must be spaced by at least four alanine residues along the peptide sequence to avoid intraloop lysine−lysine interactions. (3) Peptides with a high Ala/Lys ratio are likely to require capping regions that solubilize and inhibit aggregation. To ensure uniform properties, all peptides in the set must bear identical N- and C-caps. (4) Within these caps, charged or polar residues must be distanced by spacing elements from the alanine-rich test core to minimize strong and unpredictable helix-stabilizing effects.[16,17a,c,23,26] (5) To maximize the relevance to biological examples the peptides should be constructed entirely from the twenty common protein-derived natural amino acids. The following three peptides meet these conditions:

peptide 1K: $YKG_3A_8KA_9G_3K\text{-}NH_2$

peptide 2K: $YKG_3A_5KA_5KA_6G_3K\text{-}NH_2$

peptide 3K: $YKG_3A_4KA_4KA_4KA_3G_3K\text{-}NH_2$

To avoid the influence of multiple charges near the helix termini, the capping regions of peptides 1K, 2K, and 3K were each designed to contain only one lysine residue, with a single tyrosine as a UV reporter at the N-terminus, sited at maximal separation from the alanine cores. Three sequential glycine residues space the charged capping termini from the core. At the C-terminus, two of these glycines may serve as a helix terminator as well as isolating elements.

Peptides 1K, 2K, and 3K each contain an 18-residue alanine-rich core within which the lysine residues are separated by at least 4 residues. Core lysines are also separated by at least three alanines from the glycine regions to maximize their siting within the center regions of long helical conformations. The long core alanine sequence of 1K is interrupted by only one lysine residue, which is positioned centrally to minimize the length of each long alanine sequence. To maintain the KA_4K spacing motif and to meet the N- and C-capping conditions, the core of the tri-Lys peptide thus must contain at least 18 residues, and three peptides are needed to achieve a maximum variation in Ala/Lys. For 1K, 2K, and 3K, the variation is 17/5 or 3.4-fold. For their size, these peptides are unique in meeting the above conditions.[27]

Aggregation States for Peptides 1K, 2K, and 3K; CD and Ultracentrifugation Results. Peptides 1K, 2K, and 3K were prepared by solid-phase peptide synthesis, purified by HPLC, and characterized by amino acid analysis and MALDI MS. Though soluble in water at concentrations approaching millimolar, 1K aggregates significantly above the low-micromolar range, and freshly prepared solutions of 2K also exhibit properties consistent with the presence of aggregates. Changes in circular dichroism (CD) spectra upon dilution, warming, and aging were initially used to probe the aggregation properties of 1K, 2K, and 3K. After these preliminary properties were established, the state of aggregation was defined by equilibrium ultracentrifugation of key samples obtained in the course of the CD studies.

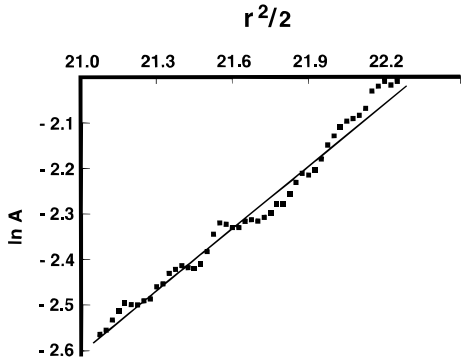

Figure 1. Analytical ultracentrifugation data for peptide 3K, 2.2 μM in 0.01 M NaCl at 2 °C; rotor speed 43 000 rpm. *A*, optical density; *r*, radial rotor distance in cm. Filled squares are averages of 8−10 raw data points; the line corresponds to a linear least-squares fit to the data, with observed slope of 0.49. Calculated slope for a monomer M = 2.2 × 10^3 D, 0.52; calculated mw for a slope of 0.49, 2.1 × 10^3 D.

Peptides that assume largely helical, sheet, or random coil conformations exhibit signature CD spectra.[28] The spectra of helices are the most intense and uniform and are characterized by a strongly positive ellipticity maximum in the region of 190 nm and a pair of strongly negative minimums at 207−210 and 220−223 nm.[28a−d] Spectra of sheets can vary substantially, but generally exhibit an ellipticity maximum near 195 nm and a single minimum near 215 nm.[28a−c] Random coil spectra show the greatest variation, but generally share a moderately strong minimum near 190 nm.[28a,c,e−h] When per residue molar ellipticities [θ] are compared, maximums and minimums of highly stable helices are invariably more intense than those of their sheet and random coil counterparts.

As expected from the close analogy between its sequence and that of characterized literature peptides,[20] the peptide 3K shows a classically helical CD spectrum at 2 °C in water, and the intensity of its ellipticity at 222 nm is unchanged after dilution over concentrations in the CD-useful range of 2−20 μM. The linearity of plots of ln *A* vs $r^2/2$ obtained from ultracentrifugation experiments carried out on peptide 3K (Figure 1) and the agreement of the resulting slope with that calculated for a monomeric model[29] together exclude the presence of significant aggregation for 3K, as expected from its literature precedents.[20]

Solutions of peptide 2K that have been diluted to concentrations below 10 μM, briefly heated to 60 °C, and aged for a few

(26) (a) C. Liu, L.-P.; Li, S.-C.; Goto, N. K.; Deber, C. M. *Biopolymers* **1996**, *39*, 465−470. (b) Sicherl, F.; Yang, D. C. *Nature* **1995**, *375*, 427−431.

(27) Further discrimination between the helix-stabilizing effects of alanine and lysine could in principle result from study of a new peptide set containing 1−4 lysine residues and involving 24-residue core sequences $A_4KA_4KA_4KA_4KA_4$, $A_5KA_5KA_5KA_6$, $A_8KA_6KA_8$, and $A_{11}KA_{12}$ with A/K of 5, 7, 11, and 23, respectively, a 4.6-fold variation, provided the monolysine peptide is included. However our experimental results for 1K suggest that the aggregation properties of peptides with core A/K > 17 are likely to require CD measurements at submicromolar concentrations that will seriously compromise the precision of the study.

(28) (a) Greenfield, N.; Fasman, G. D. *Biochemistry* **1969**, *8*, 4108−4116. (b) Yang, J. T.; Wu, C.-S. C.; Martinez; H. M. *Methods Enzymol.* **1986**, *130*, 208−257. (c) Zhong, L.; Johnson, W. C., Jr. *Proc. Natl. Acad. Sci. U.S.A.* **1992**, *89*, 4462−4465. (d) Woody, R. W. In *The Peptides*; Hruby, V. J., Ed.; Academic Press: New York, 1995; Vol. 7, pp 16−114. (e) Lord, R. S.; Cox, D. J. *Biopolymers* **1973**, *12*, 2359−2373. (f) Mattice, W. L. *Biopolymers* **1974**, *13*, 169−183. (g) Mattice, W. L.; Harrison, W. H. *Biopolymers* **1975**, *14*, 2025−2033. (h) Toniolo, C.; Bonora, G. M. *Can. J. Chem.* **1976**, *54*, 70−76.

(29) Laue, T. M.; Shah, B. D.; Ridgeway, T. M.; Pelletier, S. L. In *Analytical Ultracentrifugation in Biochemistry and Polymer Science*; Harding, S. E., Rowe, A. J., Horton, J. C., Eds.; Royal Society of Chemistry: Cambridge, U.K., 1992; pp 90−125.

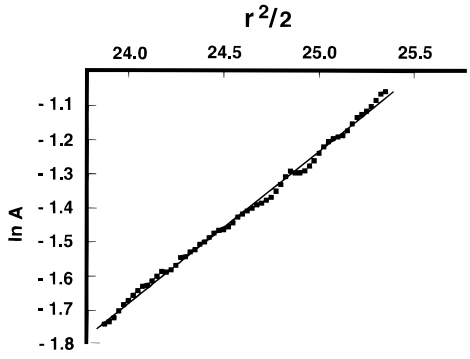

Figure 2. Analytical ultracentrifugation data for peptide 2K after heat treatment and aging (see Experimental Section), 8.7 μM in 0.01 M NaCl at 2 °C; rotor speed 43 000 rpm. *A*, optical density; *r*, radial rotor distance in cm. Filled squares are averages of 8−10 raw data points; the line corresponds to a linear least-squares fit to the data, with observed slope of 0.45. Calculated slope for a monomer M = 2.1 × 10^3 D, 0.52; calculated mw for a slope of 0.45, 1.9 × 10^3 D.

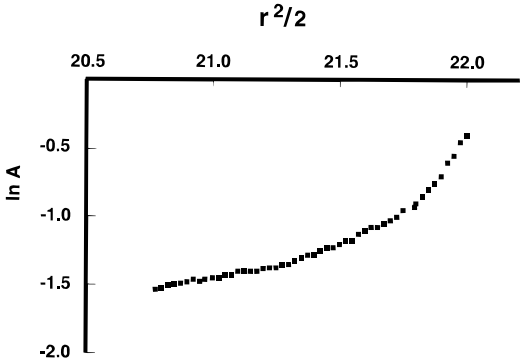

Figure 3. Analytical ultracentrifugation data for peptide 1K after brief heat treatment and aging (see Experimental Section), 1.3 μM in 0.01 M NaCl at 2 °C; rotor speed 43 000 rpm. *A*, optical density; *r*, radial rotor distance in cm. Filled squares are averages of 8−10 raw data points. The lack of linearity for this plot indicates the presence of multiple types of aggregates in the solution. The average slope in the region bounded as 20.78 < $r^2/2$ < 21.50 is 0.44, in agreement with the data of Figure 4. The average slope for $r^2/2$ > 21.70 is 2.2.

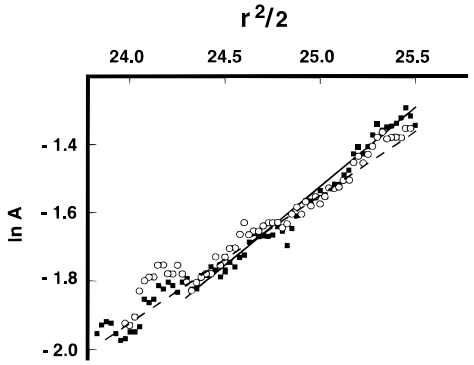

Figure 4. Analytical ultracentrifugation data for peptide 1K (unaggregated by CD criteria, see Experimental Section), 1.0 μM in 0.01 M NaCl at 2 °C; rotor speeds 40 000 (open circles) and 43 000 rpm (filled squares). Both data symbols are averages of 8−10 raw data points. *A*, optical density; *r*, radial rotor distance in cm. The dashed line corresponds to a linear least-squares fit to all of the 43 000 rpm data (observed slope, 0.40); the solid line (observed slope, 0.49) is a fit to a 43 000 rpm data set that excludes the data for $r^2/2$ < 24.25, which may be sensitive to the presence of absorbing particulates. The mean value of 0.445 is used for the calculation of molecular weights. Calculated slope for a monomer M = 2.1 × 10^3 D, 0.51; calculated mw for a slope of 0.445, 1.8 × 10^3 D.

days show analogous properties. Their CD spectra are characteristically helical and essentially invariant over the concentration range of 2.2−21.4 μM. No hysteresis changes were observed when the sample was heated to 60 °C or cooled to 2 °C. Ultracentrifugation data for peptide 2K were characteristic of an unaggregated state and were unexceptional (Figure 2).

CD spectra of freshly prepared solutions of peptide 1K at 2 °C in water in the concentration range of 1−160 μM give CD spectra that fail to correspond to those of simple peptide conformers and are dependent on sample history. At decreasing wavelengths below 205 nm all share a steeply increasing positive ellipticity and all show a single broad negative minimum at ∼217 nm (typical mean residue $[\theta]_{217}$ of ∼−10 000 deg cm^{-1} dmol^{-1}), with a width at 80% height of ∼14 nm. Although this ellipticity pattern resembles a weak β-sheet, the breadth of the minimum is atypical and suggests a significant helical contribution. Most of these spectra can be approximated from reference data[28] as roughly 50% random coil, 25% sheet, and 25% helix. Brief heating to 60 °C of these fresh solutions of 1K significantly decreases the intensity and breadth of the minimum, which is restored with only small changes upon immediate cooling. This behavior suggests rapid, reversible melting of a weak helix, with little or no change in the very significant fraction of β-structure. At low micromolar concentrations, aged solutions of 1K showed time-progressive and history-dependent ellipticity changes, primarily in the region below 220 nm.

Storage of 1K at concentrations below 2 μM for 10 days at ambient temperature with brief periods of warming generated a solution with a weak helical spectrum, characterized by double minimums at 206 and 222 nm and a positive slope below 206 nm. This spectrum was now invariant to more prolonged storage (4 months) or to 10-fold dilution, and its intensity was reproducibly diminished by heating and restored by cooling, without hysteresis effects. By CD criteria, these solutions thus appeared to contain largely unaggregated, weakly helical peptide 1K.

Ultracentrifugation established the presence of aggregates within the unaged solutions of 1K, characterized by the single broad CD minimum at 217 nm. After ultracentrifugation of the undiluted stock solution as well as freshly diluted samples, complete sedimentation was observed within the cell, in which no UV absorption remained that was attributable to peptide. Diluted, partially aged solutions typically exhibited the curved plot of ln *A* vs $r^2/2$ (*A*, optical density; *r*, radial distance) seen in Figure 3, suggesting the presence of both the monomer of 1K and oligomers. Aged solutions that were not aggregated by CD criteria all exhibited linear ln *A* vs $r^2/2$ plots upon ultracentrifugation, as typified by Figure 4. Further tests showed that the peptide 1K was not degraded during the aging process and that for aged solutions no overall concentration change occurred in the cell during sedimentation. Diluted solutions of 1K at concentrations below 2 μM that have been heated and then aged for 10 days or more contain largely unaggregated peptide.

Studies of a large number of samples of peptide 1K with differing histories show that despite the changes induced by heating and aging at shorter wavelengths, the mean residue ellipticity at 222 nm remained nearly invariant. For example, in one series, $[\theta]_{222}$ at 2 °C for the initial highly aggregated 0.15 mM stock solution was −10 800 deg cm^{-1} dmol^{-1}, and after dilution to 0.7−1.4 μM and completion of aging, it had decreased by only 11% to −9600. The ultracentrifugation experiments cannot exclude the presence of a small percentage of residual aggregate, but given the near invariance of $[\theta]_{222}$ to

the dilution and aging process, its presence would not change the fractional helicity value assigned from $[\theta]_{222}$ significantly.

Fractional Helicity; Predicted Effects of Temperature, Denaturant, and Trifluoroethanol (TFE) on the CD Spectra of Peptides 1K, 2K, and 3K. Nearly all polypeptides that exhibit helical properties in solution exist as complex manifolds made up of nonhelical as well as short and long helical conformations. The stability of the helical submanifold is usually expressed as fractional helicity fh, the fraction of the potentially helical backbone α-carbons of the peptide that appear within helical substructures. Universally, fh is calculated from the CD spectrum of the peptide as a linear function (eq 1) of

$$[\theta]_{222,\mathrm{obs}} = \mathrm{fh}[\theta]_{222\ \mathrm{helical}} \quad (1)$$

$$[\theta]_{\mathrm{helical}} = [\theta]_{222\ \mathrm{helical,\ limiting}}(1 - a/n) \quad (1a)$$

the experimental mean residue molar ellipticity $[\theta]$ at the 222-nm CD minimum. The limiting proportionality constant $[\theta]_{222\ \mathrm{helical}}$ of eq 1 is assigned a small length dependence, for which n is the overall peptide length and the constant a of eq 1a is typically given the value of 2.5.[7,20,21]

Equation 1 results if two assumptions are applied to a more rigorous expression in which the observed molar ellipticity is expressed as a mole fraction-weighted sum of molar ellipticities for all conformational subspecies. First the contributions of nonhelical residue ellipticities are neglected. Second, to convert molar ellipticities to the mean residue molar ellipticities $[\theta]$ of eq 1, a mean value of the latter is applied to conformations containing short as well as long helical regions. The $[\theta]$ correction given by eq 1a for the overall peptide length is assumed to accommodate the length variations seen within the helical subspecies.

$$[\theta]_{\mathrm{obs}} = [\theta]_{\mathrm{random}} + \mathrm{fh}([\theta]_{\mathrm{helical}} - [\theta]_{\mathrm{random}}) \quad (2)$$

Equation 2, which embodies a two-state model, is often invoked to account for the CD changes at any wavelength that result from systematic variations of temperature, [TFE], or [GuHCl]. Although two-state models are commonly used to describe the cooperative transformations of globular proteins from random coil to native conformations, their relevance to the intrinsically less well-defined states of peptide helices can be questioned. The existence of an isodichroic point at 203 nm for a series of temperature or additive-dependent CD spectra of a particular peptide is often cited as strong evidence for the relevance of a two-state model.[30,31] In fact, literature reports of such CD spectra often show diverse patterns in the 200−205-nm region. For some peptides, an isodichroic point is exceptionally well-defined.[32] For others, it is more appropriate to speak of a dichroic region, which can extend over as much as 5-nm range with a relatively large variation in $[\theta]$.[30d,33] The isodichroic point may appear outside the 203 ± 2 nm wavelength range or it may show a wide variation in $[\theta]_{203}$.[30b,34] For peptides for which the maximum intrinsic helicity is low, the value of $[\theta]_{203}$ can fall in the anomalously low range of -2×10^3 to -4×10^3 deg cm^{-1} dmol^{-1}.[35] We conclude that the presence of an isodichroic point in this region provides evidence supporting the dominance of helical and random coil ellipticities in this region, but it cannot be used as strong evidence for a two-state model, and its absence cannot be taken as proof that a poor correlation may exist between fractional helicity and $[\theta]_{222}$. However, particularly for spectra that exhibit weak $[\theta]_{222}$ signals, the quantitative assignment of helicity from ellipticity is subject to errors arising from the effects of random coil contributions at long wavelength. Prediction of the magnitude or even the sign of these from a "standard" random coil CD spectrum appears to be questionable. The $[\theta]$ values of random coil states for λ less than 215 nm exhibit substantial temperature variations, and recent evidence supports the contribution to the random coil state of weak PII left-handed helical conformations that are likely to be composition, sequence, and solvent-dependent.[36] This is a significant consideration for 1K, 2K, and 3K if the value of $[\theta]_{222}$ is observed to be small. A third of the sequence residues of these peptides appear within N- and C-caps that are expected to assume distorted helical or nonhelical conformations. The Gly_3 regions, though they are intrinsically achiral, are likely to assume induced chiral backbone conformations that result from the neighboring chiral environment.[37] At short wavelengths, the contributions of the resulting ellipticities to the CD spectra are not predictable but may depend on the degree of helicity of the alanine core and may become significant for a peptide in which the intrinsic helicity of the alanine core is low. Their contribution at $[\theta]_{222}$ is expected to be much smaller, but will nonetheless reduce the accuracy of the correlation of eq 1 if $[\theta]_{222}$ is found to lie below 10 000 deg cm^2 dmol^{-1}. It should not change the rank ordering of fractional helicities that is based on the magnitudes of $[\theta]_{222}$.

A fractional helicity approaching zero is often assumed for a peptide at high denaturant concentration (GuHCl) or at high temperature, and 100% fractional helicity has been assumed at a TFE concentration sufficient to cause a leveling in $[\theta]_{\mathrm{observed}}$. For $(Ala_nLys)_m$ peptides, recent measurements of w values show that these assumptions are unwarranted. Temperature[17] and TFE dependencies[38] of helical propensities have been reported for alanine-rich, lysine-containing peptides, and Lifson−Roig modeling shows that elevated temperatures do not abolish helicity and the presence of TFE does not eliminate the random coil state. Thus for 1K, 2K, and 3K in water at 60 °C, the likely range of fractional helicities can be calculated as 12−18%, and in water containing 12 M% TFE, the likely fractional helicity range is 55−71%. As a result, unless s_{Ala} equals s_{Lys}, the ellipticities for 1K, 2K, and 3K are not expected to converge to limiting values at high temperatures or at high [TFE]. The order

(30) (a) Scholtz, J. M.; Marqusee, S.; Baldwin, R. L.; York, E. J.; Stewart, J. M.; Santoro, M., Bolen, D. W. *Proc. Natl. Acad. Sci. U.S.A.* **1991**, *88*, 2854−2858. (b) Merutka, G.; Shalongo, W.; Stellwagen, E. *Biochemistry* **1991**, *30*, 4245−4248. (c) Lehrman, S. R.; Tuls, J. L.; Lund, M. *Biochemistry* **1990**, *29*, 4491−5596. (d) Marqusee, S. Baldwin, R. L. *Proc. Natl. Acad. Sci. U.S.A.* **1987**, *84*, 8898−8902.

(31) Holtzer, M. E.; Holtzer, A. *Biopolymers* **1992**, *32*, 1675−1677.

(32) (a) Dans, P. J. P.-C.; Lyu, C.; Manning, M. C.; Woody, R. W.; Kallenbach, N. R. *Biopolymers* **1991**, *31*, 1605−1614. (b) Dyson, H. J.; Rance, M.; Houghten, R. A.; Wright, P. E.; Lerner, R. A. *J. Mol. Biol.* **1988**, *201*, 201−217.

(33) (a) Muñoz, V.; Serrano, L. *J. Mol. Biol.* **1995**, *245*, 297−308. (b) Lazo, N. D.; Downing, D. T. *Biochemistry* **1997**, *36*, 2559−2565. (c) Shalongo, W.; Dugad, L.; Stellwagen, E. *J. Am. Chem. Soc.* **1994**, *116*, 8288−8293.

(34) (a) Kuhlman, B.; Yang, H. Y.; Boice, J. A.; Fairman, R.; Raleigh, D. P. *J. Mol. Biol.* **1997**, *270*, 640−537. (b) Jackson, D. Y.; King, D. S.; Chmielewski, J.; Singh, S.; Schultz, P. G. *J. Am. Chem. Soc.* **1991**, *113*, 9391−9392. (c) Storrs, R. W.; Trucksese, D.; Wemmer, D. E. *Biopolymers* **1992**, *32*, 1695−1702.

(35) (a) Klee, W. A. *Biochemistry* **1968**, *7*, 2731−2736. (b) Mammi, S.; Manni, N. J.; Peggion, E. *Biochemistry* **1988**, *27*, 1374−1379.

(36) (a) Park, S.-H.; Shalongo, W.; Stellwagen E. *Protein Sci.* **1997**, *6*, 1694−1700. (b) Siligardi, G.; Drake, A. F. *Pept. Sci.* **1995**, *37*, 281−287. (c) Serrano, L. *J. Mol. Biol.* **1995**, *254*, 322−333.

(37) Aurora, R.; Srinivasan, R.; Rose, G. D. *Science* **1994**, *264*, 1126−1130.

(38) (a) Cammers-Goodman, A.; Allen, T. J.; Oslick, S. L.; McClure, K. F.; Lee, J. H.; Kemp, D. S. *J. Am. Chem. Soc.* **1996**, *118*, 3082−3090. (b) Jasanoff, A.; Fersht, A. R. *Biochemistry* **1994**, *33*, 2129−2135. (c) Luo, P.; Baldwin, R. L. *Biochemistry* **1997**, *36*, 8413−8419.

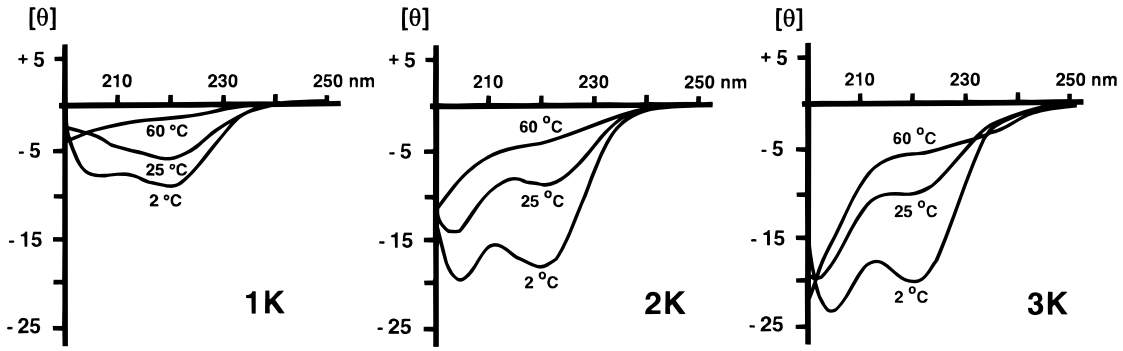

Figure 5. Mean residue ellipticities $[\theta] \times 10^{-3}$ (deg-cm^2 dmol^{-1}) for 1K, 2K, and 3K in 0.01 M NaCl pH 3.5 at 2, 25, and 60 °C and the following concentrations: 1K, 1.0 μM; 2K, 8.7 μM; 3K, 2.2 μM. As discussed in the Experimental Section, molar ellipticities were converted to $[\theta]$ values by division by 22, the length of the peptides in their helical regions. Multiplying the ordinate scales of Figures 5−7 by 22/27 does not affect the key comparison of relative helicities.

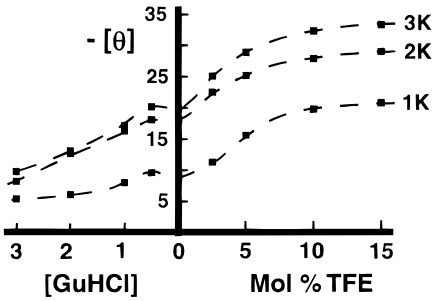

Figure 6. Mean residue ellipticities $[\theta] \times 10^{-3}$ (deg cm^2 dmol^{-1}) at 222 nm for 1K, 2K, and 3K at 2 °C in aqueous solutions of TFE and GuHCl.

of fractional helicities for 1K, 2K, and 3K seen at 2 °C is expected to persist at higher temperatures or in the presence of TFE, but with a substantial decrease in the differences in ellipticity between series members.

Experimental Results of Helicity Measurements for 1K, 2K, and 3K

Figure 5 shows CD spectra for 1K, 2K, and 3K at aggregation-free concentrations in water at 2, 25, and 60 °C. Figure 6 shows $[\theta]_{222}$ for these peptides in aqueous solution at 2 °C as a function of the concentration of GuHCl or TFE. Each peptide shows the expected, characteristic sigmoid TFE titration curve[38] with maximum response to TFE in the mole percent range of 2−6, and a leveling beyond 10. Relative to its value in water, peptide 1K in 15 mol % TFE shows a 2.3-fold increase of $-[\theta]_{222}$; but the corresponding value for peptide 3K is only 1.66-fold. The greater sensitivity of peptide 1K to TFE implies a significantly greater TFE-induced increase in w_{Ala} relative to w_{Lys}. The difference in $[\theta]_{222}$ that is observed for the three peptides at 2 °C and 15 mol % TFE is consistent with the prediction from measured w_{Ala} values.[39]

At 0.5 M GuHCl, all three peptides exhibit the slight increase in $-[\theta]_{222}$ that is expected for an increase in ionic strength at low salt.[21a,40] At higher GuHCl concentrations, substantial denaturation occurs and $-[\theta]_{222}$ for the three peptides decreases, although significantly, the slope of the decrease is smaller for peptide 1K, consistent with a reported relative insensitivity of polyalanine sequences to denaturants.[41] Extrapolation of the experimental denaturation curves suggests that the three peptides may converge to a common ellipticity value at ∼6−8 M [GuHCl], at which accurate $[\theta]$ values for peptide 1K were not measurable.

The most significant experimental results of this study are the $[\theta]$ measurements of Figure 5 at 2 °C, where maximum helicity is expected. All three peptides show evidence of an isoellipsoidal point close to 200 nm, and we attribute the significant variation in $[\theta]_{200}$ that is seen between 1K, 2K, and 3K to short-wavelength sequence-specific contributions of the capping regions to the spectra of the random coil states as well as to contributions of highly populated sequence-specific random coil ellipticities to the spectrum of 1K. The similarities between the CD spectrum of 1K and those of other weakly helical peptides[35] are significant. Likewise, part of the variation of the weak signals observed for $[\theta]_{222}$ in the 60 °C spectra doubtless reflect random coil contributions as well as intrinsic *w* value-attributable variations in fractional helicity.

These details notwithstanding, the CD spectra of 1K, 2K, and 3K at low temperatures are helical, the rank ordering of $[\theta]_{2ss}$ at 2 °C for the three peptides is unambiguous, and their 222-nm minimums become less intense with an increase in Ala/Lys. The stability of helices formed by A_nK peptides must be primarily attributed to large w_{Lys} values that appear in alanine-rich contexts and not to an intrinsic helical propensity of alanine residues.

Discussion

Given a helical CD spectrum for a polypeptide of length *n*, its fractional helicity is usually taken as proportional to its mean residue molar ellipticity at 222 nm, $[\theta]_{222}$, as shown in eq 1. Provided the helix initiation parameter v and helical propensities *w* for the constituent amino acids are known, the Lifson−Roig algorithm can be used to estimate the fractional helicity and from it the $[\theta]_{222(calcd)}$. Figure 7a compares the observed ellipticities at 2 °C for peptides 1K, 2K, and 3K with ellipticities calculated using the Doig and Baldwin modification of the Lifson−Roig algorithm and the *w*, v, and capping parameters of Doig and Baldwin.[24b,c] Substitution of *w* values calculated from our reported temperature- and context-dependent s_{Ala} and s_{Lys} values[17] results in the quantitative correlation of Figure 7b. For Figure 7b but not for a, the differences between calculated and experimental ellipticities fall within the accuracies of the measurements and calculations. The *w* values we have assigned from study of N-templated peptides uniquely model the helical properties of significantly larger nontemplated Ala-Lys peptides.

(39) The observed ellipticities for all three peptides in 15 mol % TFE can be modeled approximately by triplets of w_{Ala}, w_{Lys}, and w_{Gly} in the respective range of 1.25, 8.0, and 0.4 to 1.4, 6.5, and 0.6.

(40) von Hippel, P. H.; Wong, K.-Y. *J. Biol. Chem.* **1965**, *246*, 3909−3923.

(41) (a) Gratzer, W. B.; Doty, P. *J. Am. Chem. Soc.* **1963**, *85*, 1193−1197. (b) Creighton, T. E. *J. Mol. Biol.* **1979**, *129*, 235−264. (c) Nozaki, Y.; Tanford, C. *J. Biol. Chem.* **1970**, *245*, 1648−1652.

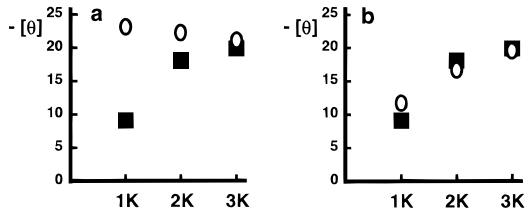

Figure 7. Comparisons of experimental values of mean residue ellipticities $[\theta] \times 10^{-3}$ (deg cm^2 dmol^{-1}) at 222 nm for 1K, 2K, and 3K at 2 °C in 0.01 M NaCl pH 3.5 (filled squares) with values calculated from *w* values using an N- and C-capping Lifson−Roig algorithm.[24] (a) Comparison with $[\theta]_{222}$ calculated using *w* values of Doig and Baldwin[24b,c] (open ellipses); (b) comparison with $[\theta]_{222}$ calculated using *w* values from Renold et al.[17b] (open ellipses).

Our assignment of an w_{Ala} value close to 1.0 finds precedent in earlier reports of Scheraga et al., who studied a variety of block and random alanine-rich copolymers.[3,42] Moreover, recently Holtzer and Hawkins have resolved a controversy concerning the properties of polyglutamic acid by noting that the older w_{Glu} values but not the values of Chakrabartty et al.[7] permit accurate modeling of the helicity of poly(glutamic acid) in water.[43] Because the peptides that comprised the database for the Chakrabartty assignments are alanine-rich and usually contain multiple lysine residues, reassignment of the w_{Ala} and w_{Lys} values and clarification of their implicit context sensitivities are likely to change other *w* values determined for this data base.

What is the significance of the variance in w_{Ala} measured from our work and from most other recent host−guest studies, and what are the implications of the existence of mutually exclusive helicity parameters for the simple test case of the alanine-rich lysine-containing peptides? Lifson−Roig modeling[25] of peptide 3K as a typical representative of this class provides some insight into these questions. Setting $\upsilon = 0.048$ for the Lifson−Roig initiation parameter and modeling all fractional helicities as equal to those calculated for the Chakrabartty *w* values ($w_{Ala} = 1.61$; $w_{Lys} = 0.82$) constrain the mean *w* value for all amino acids to 1.42, which provides a useful characterization of the helicity peculiar to the local structure of this and similar peptides. Apportioning this mean *w* value differently between lysine and alanine can generate the parameters of Chakrabartty et al.[7] or those of Renold et al.[17b] Each of these parameter sets can be viewed as an optimized descriptor of the dependence of the helicity on amino acid composition for a particular class of polypeptides that is characterized by implicit context dependences. Viewed in this way, the correlation that has been reported between the Chakrabartty parameters and the stability changes induced by protein site mutations[11] implies that the Chakrabartty *w* values share the implicit context dependencies with helical environments found in at least some natural proteins. Sets of *w* values that have been optimized for commonly encountered protein contexts may be valuable predictive tools, but it is important to realize that these are only approximations that are tied to a particular data set, however large. The limiting precision of protein helicity predictions that can be achieved solely by such optimized *w* value sets, without site and context corrections, is currently unknown, but this precision is clearly an important characterizing variable for such helical modeling studies.

Valuable though empirical approaches of this type may be, they beg the question of the causal factors that govern the helicity of polypeptides. To address causality, one must examine the proper apportioning between all independent factors that govern helicity, and only at this level can one construct a predictive helicity algorithm that is based on a rational chemical understanding of the underlying energetic effects.

The analysis of the three peptides of this study is part of an ongoing investigation in our laboratories aimed at developing this rational chemical understanding. The ^{1}H NMR reporter function of Ac-Hel$_1$ N-templated peptides is being used to augment and calibrate the CD-based helicity scale, to test the underlying assumptions and expand the scope of Lifson−Roig helicity algorithms, and to evaluate the relative weights of context-dependent, site-dependent, and context-independent contributions to the helicities of medium-sized polypeptides. These issues are all directly pertinent to the ongoing debate concerning the origins and nature of polypeptide helicity. A key preliminary question is, why should one expect N-templated small peptides to be satisfactory models for the properties of larger nontemplated peptide helices? The structural and energetic factors that define C-terminal end effects are keys to addressing this question.

Using N-templated peptide conjugates, we have previously reported an attempt to distinguish the helical propensities at the C-terminus of a helix from those in the core.[19c] Within the error limits of the analysis, no difference could be detected. In this early study, only very short helix lengths were examined, but we have also failed to observe statistically significant differences for a larger set of *w* values measured in both short- and medium-sized templated peptides.[17a,c]

The C- and N-termini are likely to behave differently with respect to the magnitude of end effects. A polypeptide helix is decidedly asymmetric, in that the backbone ϕ and ψ dihedral angles orient the side chain of an amino acid residue close to the helix core, away from the C-terminus and toward the helix N-terminus.[44] The side-chain functions of amino acid residues at the helix N-terminus are more likely to interact with the NH functions of N-terminal amides than with the helix barrel, but extended side chains of residues at the C-terminus can naturally pack against the barrel.[14,45] For the extended side chains of lysine and arginine, such packings have been predicted by molecular mechanics studies and verified by ^{1}H NMR NOE investigations[16,17a] and by X-ray crystallography.[26b] Significantly, we have documented large helical stabilizations for these residues.[17] If one models the energetics of a helical propensity as comprising backbone entropic and hydrogen-bonding effects, together with the effects of side-chain entropic restraints[9] and hydrophobic and electrostatic packing stabilizations,[14] then the latter are found to be substantially present for both core and C-terminal helical amino acid residues, while the former are constant factors in any peptide series and likely to be subsumed within the general helicity parameters. Thus, it is not surprising that helicity parameters derived from short N-templated peptides model the helicities of much larger nontemplated peptides.

This analysis demonstrates a fundamental limitation of the Ac-Hel$_1$ conjugates. No N-templated peptide conjugate can

(42) (a) Ingwall, R. T.; Scheraga, H. A.; Lotan, N.; Berger, A.; Katchalski, E. *Biopolymers* **1968**, *6*, 331−368. (b) Vila, J.; Williams, R. L.; Grant, J. A.; Wójcik, J.; Scheraga, H. A. *Proc. Natl. Acad. Sci. U.S.A.* **1992**, *89*, 7821−7825.

(43) (a) Holtzer, A. *J. Am. Chem. Soc.* **1994**, *116*, 10837−10838. (b) Spek, E. J.; Gong, Y.; Kallenbach, N. R. *J. Am. Chem. Soc.* **1995**, *117*, 10773−10774. (c) Holtzer, A.; Hawkins, R. B. *J. Am. Chem. Soc.* **1996**, *118*, 4220−4221.

(44) (a) Presta, L. G.; Rose, G. D. *Science* **1988**, *240*, 1632−1641. (b) Pauling, L.; Corey, R. B. *Proc. Natl. Acad. Sci. U.S.A.* **1951**, *37*, 241−250.

(45) (a) Doig, A. J.; MacArthus, M. W.; Stapley, B. J.; Thornton, J. M. *Protein Sci.* **1997**, *6*, 147−155. (b) Forood, B.; Feliciano, E. J.; Nambiar, K. P. *Proc. Natl. Acad. Sci, U.S.A.* **1993**, *90*, 838−842. (c) Gong, Y.; Zhou, H. X.; Guo, M.; Kallenbach, N. R. *Protein Sci.* **1995**, *4*, 1446−1456.

model the special interactions that arise between the amide NH functions and amino acid side chains at the N-terminus of a nontemplated peptide helix. Studies of peptides linked to as yet unavailable C-terminal reporting templates should address this problem and should complement the helical analyses that result from study of N-templated peptides.

Context-dependent helix stabilizations have been documented and quantitatively analyzed for classes of stabilizing interactions between amino acid side chains at (i, $i + 4$) and (i, $i + 3$) sites within a helical loop. These include salt bridges,[46] hydrogen-bonding interactions,[47] hydrophobic contacts,[48] and π-cation interactions.[49] More subtle context effects have not been quantitatively analyzed but may have comparable energetic significance. Steric crowding at one amino acid site may interfere with helix-stabilizing packing of a neighboring amino acid side chain with an extended linear structure, such as that of lysine, arginine, glutamic acid, glutamine, and methionine. Stabilization of the random coil state by sequence-specific hydrophobic and electrostatic contacts between pairs of side chains may result in apparent helix destablization. Alanine-rich short peptide helices have been analyzed by Millhauser et al. as rapidly equilibrating manifolds of both α and 3_{10} structures.[22] In such a manifold, a w value must correspond to the helical propensity of a given amino acid within an abundance-weighted average of 3_{10} and α contexts, and an amino acid that selectively stabilizes and strongly disposes a local helix toward one of these structures may alter the w values of neighboring amino acids. Finally, most helix-stabilizing amino acids exhibit only marginal helical propensity, and the helices they generate are consequently locally fragile structures, potentially subject to structural deformation. A strong local helix stabilizing factor, such as an (i, $i + 4$) Phe−His π-cation interaction,[49] has the potential to override both local helical energetics and geometry and may introduce its own local distortions within contiguous helical structure. The w values for other amino acid residues that are measured in such locally stabilized contexts may therefore reflect the degree to which these residues facilitate or hinder this distortion.

Although several of the above effects may contribute, the likely explanation for the large w values we have observed for Lys and Arg in an alanine-rich context is a significant local hydrophobic and electrostatic stabilization of the helix, resulting from a temperature-dependent packing of the side chain against the helix barrel. Packing of this type is expected to be optimized by the presence of neighboring helix-stabilizing amino acids that minimize steric crowding in the immediate vicinity of the packed side chain, particularly at the ($i - 3$, i) and ($i - 4$, i) sites. Alanine is expected to be the ideal noninteractive partner for the helix-stabilizing amino acids with packable side chains. Assignments of w values for alanine-rich host contexts that contain implicit stabilizations by these amino acids will inevitably place w_{Ala} at or near the top of the list.

Summary and Consequences

We have shown that for three medium-sized helical peptides 1K, 2K, and 3K that differ only in the number of widely spaced lysine residues present in an alanine-rich region, the fractional helicity increases with the number of lysine residues, not with the number of alanines. This result is contrary to the predictions based on most recently tabulated helical propensities, but it is consistent with predictions based on w values we have assigned for small peptides linked to the reporting helical template Ac-Hel_1. Although this finding needs to be generalized, it validates our template approach to the quantitation of helicity.

The helical manifolds formed by small N-templated peptides are intrinsically simpler than those formed by larger peptides in which helix initiation occurs randomly, and study of these systems has the potential for more incisive characterization of the separable factors that influence helicity. Realization of the full potential of the reporting template principle will require calibration of the CD-based scale of helicity against the NMR-based scale of the Ac-Hel_1 conjugates. It will also require development of a self-consistent set of satellite helical reporters that can be positioned at local sites within the peptide sequence. These should substantially increase the resolution of both CD and Ac-Hel_1 helicity assignments.

The large w values we have measured for lysine and arginine in alanine-rich contexts suggest that structural redesign of the amino acids with flexible side chains bearing polar termini (Lys, Arg, Glu, Gln) can be used to generate unnatural amino acids with less flexible side chains that can achieve greater local helical stabilization through optimized hydrophobic and electrostatic interactions with the helix core.

Polypeptide helices are manifolds of all possible helical conformations, and their rapidly equilibrating averages behave as frayed structures whose stability is very sensitive to local amino acid substitutions. Synthesis of superhelical amino acid analogues and their incorporation at the N- and C-termini of natural peptide sequences may make possible the routine synthesis of peptide analogues that can be satisfactorily described as assuming single, 100% helical conformations. Such analogues are likely to be potent research tools at a variety of significant interfaces between chemistry and biology.

Experimental Section

1. Synthesis and Purification of Peptides. The peptides 1K, 2K, 3K were prepared by manual solid-phase synthesis using a standard 9-fluorenylmethoxycarbonyl (Fmoc) strategy on Knorr resin (Fmoc-2,4-dimethoxy-4′-(carboxymethyloxy)benzhydrylamine linked to aminomethyl resin, Advanced ChemTech) with a loading of 0.85 mequiv/g. Fmoc-Lys(Boc)-OH, Fmoc-Gly-OH, Fmoc-Ala-OH, and Fmoc-Tyr(tBu)-OH were purchased from Novabiochem. Methanol and dichloromethane were Mallinckrodt AR grade; *N*,*N*-dimethylformamide (DMF) was Burdick & Jackson Brand high-purity solvent. All other chemicals were purchased from Aldrich and used as received. Coupling was performed overnight at ambient temperature with a mixture of 3 equiv of Fmoc-protected amino acid, 3 equiv of 1-hydroxybenzotriazole, and 3 equiv of 1,3-diisopropylcarbodiimide in DMF. Coupling efficiency was monitored by the Kaiser ninhydrin test,[50] and couplings were repeated several times if necessary. The introduction of a Lys residue to long Ala sequences (6 or 9 Ala residues) proved to be extremely difficult and required five to eight recouplings. After each elongation step, a capping mixture of acetic anhydride and pyridine

(46) (a) Marqusee, S.; Baldwin, R. L. *Proc. Natl. Acad. Sci. U.S.A.* **1987**, *84*, 8898−8902. (b) Stellwagen, E.; Park, S.-H.; Shalongo, W.; Jain, A. *Biopolymers* **1992**, *32*, 1193−1200. (c) Huyghues-Despointes, B. M. P.; Baldwin, R. L. *Biochemistry* **1997**, *36*, 1965−1970.

(47) (a) Scholtz, J. M.; Qian, H.; Robbins, V. H.; Baldwin, R. L. *Biochemistry* **1993**, *32*, 9668−9676. (b) Huyghues-Despointes, B. M. P.; Klingler, T. M.; Baldwin, R. L. *Biochemistry* **1995**, *24*, 13267−13271.

(48) (a) Nemethy, G.; Scheraga, H. A. *J. Phys. Chem.* **1962**, *66*, 1773−1789. (b) Vasquez, M.; Scheraga, H. A. *Biopolymers* **1988**, *30*, 121−134. (c) Padmanabhan, S.; Baldwin, R. L. *J. Mol. Biol.* **1994**, *241*, 706−713. (d) Viguera, A. R.; Serrano, L. *Biochemistry* **1995**, *34*, 8771−8779. (e) Zerkowski, J. A.; Powers, E. T.; Kemp, D. S. *J. Am. Chem. Soc.* **1997**, *119*, 1153−1154.

(49) (a) Armstrong, K.; Fairman, R.; Baldwin, R. L. *J. Mol. Biol.* **1993**, *230*, 285−291. (b) Loewenthal, R.; Sancho, J.; Fersht, A. R. *J. Mol. Biol.* **1992**, *224*, 759−770. (c) Dougherty, D. A. *Science* **1996**, *271*, 164−168. (d) Fernández-Recio, J.; Vásquez, A.; Civera, C.; Sevilla, P.; Sancho, J. *J. Mol. Biol.* **1997**, *259*, 184−197.

(50) Stewart, J. M.; Young, J. D. *Solid-Phase Peptide Synthesis*; Pierce Chemical Co.: Rockford, IL, 1984; pp 105−106.

(1:1, v/v) was applied. The last residue coupled to each peptide was Tyr to serve as a UV tag for identification and concentration determination of the full-length peptide. Cleavage from the resin was achieved using a 90:5:5 (v/v/v) trifluoroacetic acid (TFA)/water/thioanisole mixture to yield N-terminal free-amine and C-terminal amide peptides. After filtration and concentration in vacuo, the residues were taken up in water. Addition of small amounts of acetonitrile was necessary to obtain clear solutions and to keep the volumes of the crude peptide solutions small.

Analytical and preparative HPLC separations were performed on a Rainin Dynamax SD-200 system equipped with a two-channel Rainin Dynamax UV-D II detector and Rainin Dynamax HPLC Method Manager Software. For analytical separations, a Vydac reversed-phase C18 column type 218TP54 was used. For preparative separations, a Vydac reversed-phase C18 column type 218TP1022 was used. HPLC solvent A was composed of Millipore high-purity water containing 0.1% TFA, while solvent B was acetonitrile (Mallinckrodt ChromAR HPLC). UV optical density of the eluent was recorded at 214 and 275 nm (tyrosine chromophore). In an initial preparative HPLC separation, those peaks with identical profiles at both wavelengths were collected and analyzed by mass spectrometry to identify the product peak. In preparative HPLC separations, portion-wise separation was necessary due to low solubility of the crude material (8−16 injections). After concentration of the combined fractions in vacuo, the residue was taken up in pure water. The product peak was divided into three fractions, representing beginning, middle, and end of the peak profile. These peptide solutions were analyzed by mass spectrometry and amino acid analysis, and for each peptide, one solution of high purity was obtained that showed a single peak by analytical HPLC (>95% pure).

Peptide 1K. Preparative HPLC separation was carried out using 12 mL/min, 0−100% solvent B over 40 min. (Analytical HPLC: 1 mL/min, 0−30% solvent B over 40 min; retention time, 37.5 min).

Peptide 2K. Preparative HPLC separation was carried out using 12 mL/min, 0−30% solvent B over 40 min. (Analytical HPLC: 1 mL/min, 0−30% solvent B over 40 min; retention time, 33.7 min).

Peptide 3K. Preparative HPLC separation was carried out using 12 mL/min, 0−30% solvent B over 40 min. (Analytical HPLC: 1 mL/min, 0−30% solvent B over 40 min; retention time, 29.0 min).

2. Characterization and Concentration Determination. A stock solution was prepared for each HPLC-purified peptide that showed a single peak in analytical HPLC (>95% pure by peak integration). MALDI mass spectral analysis of dilute samples of these stock solutions gave the following molecular weights: K1, calculated $[M + H^+] = 2115.142$, found $[M + H^+] = 2115.12$; K2, calculated $[M + H^+] = 2172.200$, found $[M + H^+] = 2171.84$; K3, calculated $[M + H^+] = 2229.257$, found $[M + H^+] = 2229.17$. For all three peptides, the molecular ion peaks showed a >95% higher intensity than all other detected peaks in the spectra. Peptide composition was confirmed by amino acid analysis of dilute samples of the three stock solutions.

Peptide concentrations required for quantitation of CD ellipticities were measured by three different methods, amino acid analysis, UV absorption, and calibrated ninhydrin analysis: Amino acid analysis (AAA) was performed on peptide solutions in the concentration range of 2−100 μM. The concentration of the three stock solutions was determined by analysis of dilute samples and showed a reproducibility of 4%. AAA was also performed on selected solutions after CD measurement to confirm the concentrations calculated for these solutions from the known stock solution concentrations and dilution factors.

An N-terminal Tyr was added to the sequence of all three peptides to allow concentration determination by UV absorption,[51] which was monitored on a Hewlett-Packard 8453 UV−visible spectrophotometer using HP ChemStation software and Hellma QS 1 cm quartz cells. Absorptions at 275 nm for the three peptide stock solutions were measured in 6 M guanidinium hydrochloride solution at concentrations from 40 to 100 μM; no evidence of light scattering was noted. In a 1-cm cell, reliable absorption data (optical density >0.06) could not be obtained for solutions more dilute than 30 μM. For each peptide, the concentration determined by UV was consistently higher than that obtained by the other two methods, which were in agreement within experimental error. The discrepancy was approximately 20−30% for peptides 2K and 3K but was greater for peptide 1K (60%), A likely source of this difference is sensitivity of the tyrosine chromophore to the state of aggregation of 1K. At the high concentrations required for the optical density measurements, even in the presence of GuHCl, 1K appears to be largely present as soluble aggregate.

Peptide concentrations were independently determined by ninhydrin colorimetric assay (NCA) following a detailed procedure developed in these laboratories.[52] Ninhydrin required for the assay (ninhydrin monohydrate, Pierce) was recrystallized twice from water prior to use, and ninhydrin stock solutions in ethylene glycol monomethyl ether were discarded after 2 weeks. Typically, a peptide solution (50−100 μL) in the concentration range of 20−40 μM was hydrolyzed (HCl/propionic acid 1:1, 150 °C, 60 min) in a degassed, Teflon-sealed tube. The hydrolysate was concentrated in vacuo, the residue was dissolved in water (300 μL), and aqueous acetate buffer containing NaCN (10 mM) (0.2 M, 300 μL) was added.[53] To this was added a solution of purified ninhydrin (168 mM, 300 μL) in peroxide-free ethylene glycol monomethyl ether. After heating (100 °C, 15 min) and cooling (10 min), the colored solution (containing Ruhemann's purple) was diluted with 2-propanol/water 1:1 (2.60 mL) and the visible optical density A was measured ($\lambda = 570$ nm) on a Carl Zeiss spectrophotometer PMQ II, using Hellma QS 1-cm quartz cells. The absorption of the peptide samples was corrected for the absorption of a blank sample obtained by the same procedure but lacking peptide. Concentrations were assigned using visible calibration curves obtained from standard solutions of each component amino acid and other amines present in each hydrolysis mixture.[54] Separate standards at 10 different concentrations were prepared from carefully weighed samples of recrystallized, dried alanine, glycine, and lysine, and 30−40 data points were collected for each calibration graph (tyrosine was treated as alanine in the NCA calculations). Strict linearity of plots of A vs concentration was observed. NCA concentrations were determined for 18 hydrolysis solutions in the concentration range of 1−75 μM prepared from 1K, 2K, and 3K; results were in agreement with AAA within 6%. A peptide or amino acid standard of known concentration was always subjected simultaneously to the same hydrolysis procedure. Comparison of known and measured concentration was used to judge quality and reliability of the assay. Reproducibility was determined to be within 3−5%.

Considering reproducibility, amount of sample, and the applicable concentration range, we judged AAA and NCA concentration determinations to be superior to the UV method and used these values for helicity calculations.

3. Analytical Ultracentrifugation. Sedimentation equilibrium experiments were performed with a Beckman Optima XL-A centrifuge using an An-60 Ti analytical rotor and six channel center pieces. Optical density A was measured at 275 nm and at several wavelengths in the 200−215-nm region, and for each sample, a wavelength was chosen that optimized ΔA for that concentration. Cell windows were treated with Sigmacote (Sigma) before assembly. Peptide solutions in aqueous 0.01 M NaCl were analyzed in the concentration range of 1−20 μM at 2 °C and at 40 000 and/or 43 000 rpm. Equilibration was reached within 12−16 h, and usually at this point, 12 data sets were gathered per sample at three different wavelengths and 0.001-cm increments. Each data point was averaged over 10 repeats, and for the plots of Figures 1−4, the resulting data points were further averaged over a 0.0025-cm interval. Only data corresponding to A greater than 0.05 AU and less than 1.2 AU were used.

Data from ultracentrifugation runs that gave linear plots of ln A vs $r^2/2$ were fitted to a single-species model to yield an apparent σ value (σ_{obs}), where $\sigma = M(1 - \nu\rho)\omega^2/RT$ (M, monomer mw; ρ, solvent density; ν, partial specific volume; ω, angular rotar velocity.) Expected monomer σ values (σ_{calc}) were calculated with partial specific volumes

(51) Brandts, J. F.; Kaplan, L. J. *Biochemistry* **1973**, *12*, 2011−2024.

(52) Oslick, S. L. Ph.D. Thesis, Massachusetts Institute of Technology, Cambridge, MA, 1996.

(53) Rosen, H. *Arch. Biochem. Biophys.* **1957**, *67*, 10−15.

(54) (a) Harding, V. J.; MacLean, R. M. *J. Biol. Chem.* **1915**, *20*, 217−230. (b) Friedman, M.; Williams, L. D. *Bioorg. Chem.* **1974**, *3*, 267−280. (c) Sheng, S.; Kraft, J. J.; Schuster, S. M. *Anal. Biochem.* **1993**, *211*, 242−249.

based on amino acid composition as described by Laue et al.[55] Peptides were classified as largely monomeric if σ_{calc} and σ_{obs} agreed within ±15% and if the plot of residuals ($A_{obs} - A_{calc}$) vs r showed no significant deviations. An analysis of residuals can be found in the Supporting Information.

With no prior heating, solutions of peptide 3K showed a typically helical CD spectrum immediately upon dilution to the micromolar range,. Ultracentrifugation of these solutions at 22 and 2 μM showed ln A vs $r^2/2$ plots consistent with monomer (Figure 1), and after equilibration, the observed mean cell optical density A_{obs} (0.10) agreed within error with the calculated optical density from the known concentration of the sample introduced into the cell A_{obs} (0.08).

The CD spectra of solutions containing peptide 2K (<10 μM) were initially history-dependent and suggestive of β-structure, but after heating to 60 °C for 3−4 h, followed by storage for 4−5 days at 25 °C, solutions were obtained that showed invariant, reproducibly temperature-dependent helical CD spectra. Figure 2 shows a linear plot of ln A vs $r^2/2$ for one such solution ($A_{obs} = 0.26$; $A_{calc} = 0.23$). Heated and briefly aged solutions of 2K in the 2−9 μM range were largely monomeric by this criterion.

Immediate dilution of an aqueous stock solution (0.15 mM) of peptide 1K to the concentration range of 1−13 μM, followed by ultracentrifugation, resulted in complete sedimentation of the peptide. Like the CD spectra of their freshly diluted 2K counterparts, spectra of these solutions were suggestive of β-structure and history-dependent. Moreover, the 1K peptide precipitated readily on glass surfaces, and silanization of CD cells was required to achieve reproducible quantitation. Treatment of the 1K stock solution with 6−8 M GuHCl, followed by aging and dilution, resulted in only weak dissociation of the aggregate. A weak interaction of GuHCl with alanine homopolymers has been previously reported.[42a] Linear ultracentrifugation plots of ln A vs $r^2/2$ were only obtained for solutions containing <2 μM of 1K that had either been stored at room temperature for >4 months or that had been initially heated to 60 °C for several hours, then cooled, and stored for shorter periods (Figure 4). Dilution, heating, and aging were thus all required for relatively rapid dissociation of the aggregate. For the sample of 1K that gave the linear ultracentrifugation plot of ln A vs $r^2/2$ seen in Figure 3 ($A_{obs} = 0.18$; $A_{calc} = 0.15$), the solution was stored for 10 days at 25 °C after a heating period of 6−8 h at 60 °C. For the 43 000 rpm data set of Figure 4, as noted in the figure legend, the mean slope of ln A vs $r^2/2$ plots is 0.445; the corresponding mean slope for the 40 000 rpm data set is 0.377. The ratio $0.445/0.377 = 0.118$, in satisfactory agreement with the expected value of $(43/40)^2 = 0.116$. Practical factors prevented exploration of runs at higher rotor speeds, but it should be noted that, although full characterization of the degree of association of the aggregates formed by 1K is not possible from our data, the major conclusion of this study is firmly established. The major species present in the solutions of peptide 1K that yielded the ultracentrifugation results of Figure 4 and the CD data of Figures 5−7 is the monomer.

The temperature-dependent CD spectra of these solutions of monomeric 1K were characteristic of weak helices, and heating and cooling induced reproducible CD changes that were identical within experimental error with those observed for solutions of 1K aged for months without heating. To confirm that prolonged storage did not result in degradation, both amino acid analysis and a MALDI spectrum that were taken on a stock solution of 1K that had been stored in a polypropylene vial at room temperature for 8 months were identical in all significant respects with those obtained from the initial sample.

4. Circular Dichroism Measurements. CD experiments were performed on an Aviv spectrometer model CD 62DS equipped with a Neslab Coolflow CFT-33 cooling device and an Osram XBO 450-W high-pressure xenon lamp. The spectrometer was operated under a rigorously oxygen-free (<0.1 ppm) nitrogen atmosphere using an Aviv oxygen scrubber, followed by an Aviv oxygen filter cartridge. Prior to quantitative measurements on 1K, 2K, and 3K, a new lamp was installed and the instrument was serviced and calibrated by Aviv Associates. The calibration was checked before and after the series of quantitative measurements by the *d*-10-camphorsulfonic acid two-point method[56] and found to be unchanged within 2%. Signal-to-noise ratio was optimized for each sample and those conditions applied to a blank. Usually, bandwidth was set at 1.5 nm, while the full-scale setting was adjusted between 500 and 50 according to sample signal. Data collection was averaged over five repeats at 0.2-nm step size and 1-s averaging time. Spectra obtained were corrected by subtracting a suitable blank, smoothed using Aviv 62DS version 4.0s software polynomial fitting, and the average intensity in the 250−260-nm region of the corrected spectra was set to zero. Under the reasonable assumption that the N- and C-capping termini contribute insignificantly to the helical molar ellipticity at 222 nm, the residue molar ellipticity [θ] was calculated by dividing molar ellipticity by 22, the length of the alanine core and four of six glycines.

Measurements of peptide solutions were taken in the concentration range of 0.2−20 μM in high-quality strain-free quartz cells of 1, 10, and 100-mm path length (1 and 10 mm, Hellma QS; 100 mm, Hellma QS jacketed cell). The 100-mm jacketed cell was thermostated using a Haake circulating water bath. Cells were treated with Sigmacote (Sigma) before use. Peptide stock solutions were diluted with 0.01 M NaCl [Mallinckrodt U.S.P. food grade NaCl in Millipore high-purity water filtered through a 0.22-μm cellulose acetate membrane disposable sterile bottle top filter (Corning)]. Solutions in 0.01 M NaCl were slightly acidic (pH 3−5, Cole-Parmer pH meter 5982-00). Typically, dilute peptide solutions (1−2 μM) were measured in a 1-cm cell at 2, 25, and 60 °C and stored in polypropylene tubes. TFE titrations were performed with 2,2,2-trifluoroethanol 99.5+%, NMR grade (Aldrich), and guanidinium hydrochloride titrations were performed with crystalline Pierce Sequanal grade guanidinium hydrochloride. Best results were obtained by direct addition of these reagents to dilute peptide solutions that showed helical double minimums in previous measurements. To explore the effect of concentration and other variables on the ellipticity of peptides 1K, 2K, and 3K, and to rigorously exclude aggregation, a database of ~50 spectra for peptide 3K, ~100 spectra for peptide 2K, and ~150 spectra for peptide 1K was generated. As noted in the ultracentrifugation section, freshly prepared solutions of peptide 3K showed concentration- and time-independent helical CD behavior, but peptides 2K and 1K displayed concentration and time dependent CD spectra if data recording was started soon after dilution of the respective stock solutions (within hours to days). The peptides 3K, 2K, and 1K thus showed progressively more significant aggregation, but storage of dilute (1−2 μM) solutions over a period of 2−7 weeks at room temperature, including occasional heating to 60 °C for 2−4 h, produced solutions that showed concentration- and time-independent CD spectra with pronounced double minimums, indicative of helical peptide conformations. After CD characterization, samples were subjected to amino acid, ninhydrin, and analytical ultracentrifugation analyses to confirm concentrations and monomeric state of the peptide.

Owing to the low measurement concentrations necessitated by its aggregation tendencies and intrinsically small ellipticity, CD measurements on peptide 1K were made in 1- and 10-cm cells. Signal-to-noise limits introduced unavoidable measurement errors for this peptide at wavelengths below 205 nm, particularly for spectra taken at high temperature or at high [GuHCl]; however, these problems were minimal at 222 nm. Because the relative order of magnitude of $-[\theta]_{222}$ in water at 2 °C for peptides 1K, 2K, and 3K is critical for the analysis of this paper, it is useful to set a bound on this order by an analysis that does not depend on independent measurements of concentration. As noted in the text, among the three peptides, 1K shows the largest net increase in $[\theta]_{222}$ with addition of TFE. If one ignores the measured concentrations for 2K and 1K and assumes that all three peptides in 15 mol % TFE/water at 2 °C must converge to the $[\theta]_{222}$ of −33 300 deg cm^2 dmol^{-1} observed for peptide 3K, then the experimental $[\theta]_{222}$ of −20 000 deg cm^2 dmol^{-1} observed for peptide 1K in 14 mol % TFE/water implies a relative concentration of [3K]/[1K] = 33.3/−20.8 = 1.6, yielding an upper bound in water at 2 °C of $[\theta]_{222}$ (−14 600 = −9600 × 1.6) deg cm^2 dmol^{-1} for 1K. This method can only set an upper bound for the $[\theta]_{222}$ of 1K in water at 2 °C, which clearly must be at least 30% smaller than that of 3K.

(55) Laue, T. M.; Shah, B. D.; Ridgeway, T. M.; Pelletier, S. L. In *Analytical Ultracentrifugation in Biochemistry and Polymer Science*; Harding, S. E., Rowe, A. J., Horton, J. C., Eds.; Royal Society of Chemistry: Cambridge, U.K., 1992; pp 90−125.

(56) Chen, G. C.; Yang, J. T. *Anal. Lett.* **1977**, *10*, 1195−1207.

Lifson−Roig Calculations. The respective N-capping, helix propagation, and C-capping terms for the Doig et al. modification[24b,c] of the Lifson−Roig helicity algorithm are nx, wx, and cx; v is the universal initiation weight for a single helical residue; mx is the matrix corresponding to amino acid x and has the form {{wx, v, 0, 0, 0}, {0, 0, $(nx \cdot nc)^{0.5}$, cx}, {v, v, 0, 0}, {0, 0, nx, 1}} and mxo is the matrix used in calculating site helicities and has the form {{wx, 0, 0, 0}, {0, 0, 0, 0}, {0, 0, 0, 0}, {0, 0, 0, 0}}:[24c] Thus, for the 3K peptide $YKG_3A_4KA_4KA_4KA_3G_3K\text{-}NH_2$, the state sum ss is given by the vector−matrix product $va \cdot my \cdot mk \cdot mg^3 \cdot ma \cdot {}^4mk \cdot ma \cdot {}^4mk \cdot ma \cdot {}^4mk \cdot ma^3 \cdot mg^3 \cdot mk \cdot vb \cdot$, where va = {0, 0, ny, 1} and vb = {{0}, {cnn}, {0}, {1}}are end vectors in the state sum calculation, and cnn is the capping term for a C-terminal primary amide group. As explained below, essentially identical fractional helicities were obtained by calculations carried out for the 22-peptide $G_2A_4KA_4KA_4KA_3G_2$.

The fractional helicity fhz at a given amino acid site z is obtained by replacing the mz value at that site in the matrix product series by mzo, recalculating the matrix product, and dividing by the overall state sum. The fractional helicity fh was calculated by excluding the first and last residue sites and taking the mean of the remaining $(n - 2)$ sites. The exclusion of the first and last sites requires comment. Because the Doig weighting term for a particular helical conformation of a peptide assigns weights of v to the first and last amino acids that belong to the helical region, these amino acids are never assigned a w-weight; thus, fhx calculated in the above manner at the first and last sites of a peptide sequence must be zero. This anomaly has also been noted by Shalongo and Stellwagen.[57] It has the consequence for a peptide sequence of 22 residues that, even for very large test wx values (>10), a fractional helicity fh calculated over all residues cannot exceed 0.909 = 20/22 (or $(n - 2)/n$ for the general case)). An average excluding the end residues (effective $n = 20 = 22 - 2$) gives the proper fh = 1.0 for a peptide assigned uniformly large wk.

The following values taken from Doig et al.[24b,c] were used in calculating the ellipticities of Figure 7a: $v = 0.048$, wa = 1.58, na = 1.0, ca = 1.0, wk = 0.90, nk = 0.79; ck = 1.09; wg = 0.05; cg = 8.85; wy = 0.55; ny = 5.2; cy = 63.0; can = 1.3. For the ellipticities of Figure 7b, the following changes were made in the above list: wa = 1.07; wg = 0.3; and wk = 3.7−4.2 for 3K and 4.2−5.0 for 1K and 2K. The latter were obtained from the 2 °C data of Renold et al. and reflect the precision of the assignments and corrections for the N-templating effect.[17b] In this region of w-space, the cited variations in wk do not result in large changes in $[\theta]_{222calc}$. It can also be shown that, as expected, $[\theta]_{222calc}$ is nearly independent of the *n*, *c*, & *w* values assigned to Y and G, provided they are varied within plausible limits. If the varying wk used in these calculations are replaced by an average ⟨wk⟩ = 3.9, values for assigned $[\theta]_{222}$ for 3K, 2K, and 1K are respectively −19.7, −15.8, and -10.8×10^3 deg cm^2 dmol^{-1}, which may be compared with the experimental values of 2 °C of −19.9, −18.1, and − 9.1. The averaged ⟨*wk*⟩ value thus results in poorer agreement with experiment for the 2K case than is seen in Figure 7b for length-dependent wk, consistent with our previous data,[17b] which demonstrates that two Lys show a measurable destabilizing interaction, even when separated by four Ala residues. The mean residue helical ellipticity at 222 nm for 1K, 2K, and 3K was calculated as $[\theta]_{222} = -35\,400$ fh; ($-35\,400 = -40\,000(1 - 2.5/22)$, following Chakrabartty et al.).[7] See the Supporting Information for further details on the Lifson−Roig calculations.

Acknowledgment. Financial support from the NIH Grant GM 13453, from the NSF Grant 9121702-CHE, and from Pfizer Research is gratefully acknowledged. K.K. acknowledges receipt of a Feodor Lynen Fellowship from the Alexander von Humboldt Foundation. We thank Prof. Klaus Biemann for MALDI MS, the analysis M.I.T. Biopolymers Laboratory for amino acid analyses, and Prof. Peter Kim for providing access to the ultracentrifuge.

Supporting Information Available: Details of Lifson−Roig computations and residual plots for ultracentrifugation experiments with peptides 1K, 2K, 3K; (9 pages, print/PDF). See any current masthead page for ordering information and Web access instructions.

JA9801947

(57) Shalongo, W.; Stellwagen, E. *Protein Sci.* **1995**, *4*, 1161−1165.